are limited. Scheidt[46] and co-workers have investigated a series of toluene-solvated first-row transition-metal complexes of 5,10,15,20-tetraphenylporphyrins. The interaction between the toluene and the metalloporphyrin involves both the central metal atom and a pyrrole ring. Schmitt's[47] perylene-bis[*cis*-1,2-bis(trifluoromethyl)ethene-1,2-dithiolato]nickel, perylene-Ni(tfd)$_2$, complex has the π base situated symmetrically above the nickel thiolate, indicating direct metal atom-π-donor interaction.

Perhaps the most intriguing indication of an interaction between benzene and the copper-ketimine complexes is that the Cu-Cu distance in the binuclear complex decreases monotonically with increasing numbers of benzenes (Table IX). The Cu-Cu distance of 3.083 (1) Å for Cu$_2$(PAApr)$_2$ is the longest reported for any binuclear copper-ketonate complex[14,23-25,48] and is the only binuclear copper complex of this type completely lacking any significant axial interaction. Of the known five-coordinate copper-ketonate complexes with σ-donor axial ligands,[49] the range of Cu-Cu distances is 3.04-3.06 Å. The Cu-Cu distances for the benzene solvated structures summarized in Table IX are very similar to the five-coordinate copper binuclear ketonates with σ-axial ligands. One other geometric parameter that significantly changes throughout the solvated complexes tabulated above is the Cu-O(trans N) length. It varies 7σ from the doubly solvated complex to the nonsolvated complex. As expected this length varies in the same direction as the Cu-Cu distance, although not so dramatically. Interestingly, it is the bridging oxygen atom that is centered in the projection of the Cu$_2$(PAAet)$_2$ complex onto the benzene plane (Figure 3), implying that this site is especially important in the π-molecular interaction.

Acknowledgments are made to the National Science Foundation (Grant CHE841-19100) for the purchase of a Syntex automated diffractometer and to the United States Air Force (Grant N00014-84-G-0211) for the purchase of a QE-300 multinuclear magnetic resonance spectrometer. The National Science Foundation (Grant CHE8300251) and the donors of the Petroleum Research Fund, administered by the American Chemical Society, are also acknowledged for the general support of this research. K.A.R. acknowledges support in the form of a Graduate Professional Opportunities Prgram Grant (GPOP).

Registry No. H_2PAA, 66734-21-2; Cu$_2$(PAAet)$_2$, 102869-03-4; Cu$_2$(PAAet)$_2$·$^1/_2C_6H_6$, 111769-79-0; Cu$_2$(PAApr)$_2$, 111742-38-2; Cu$_2$(PAAan)$_2$, 85319-02-4; Cu$_2$(PAApnan)$_2$, 85319-03-5; bis[2,2-dimethyl-7-(methylimino)-3,5-octanedionato]dicopper(II), 111742-45-1; bis[2,2-dimethyl-7-(butylimino)-3,5-octanedionato]dicopper(II), 111742-39-3; bis[2,2-dimethyl-7-(*p*-methylphenylimino)-3,5-octanedionato]dicopper(II), 111742-41-7; bis[2,2-dimethyl-7-(*p*-methoxyphenylimino)-3,5-octanedionato]dicopper(II), 111742-40-6; bis[2,2-dimethyl-7-(*p*-chlorophenylimino)-3,5-octanedionato]dicopper(II), 111742-42-8; bis[2,2-dimethyl-7-(*p*-bromophenylimino)-3,5-octanedionato]dicopper(II), 111742-44-0; bis[2,2-dimethyl-7-(*p*-(trifluoromethyl)phenylimino)-3,5-octanedionato]dicopper(II), 111742-43-9; methanamine, 74-89-5; ethanamine, 75-04-7; propanamine, 107-10-8; butanamine, 109-73-9; aniline, 62-53-3; *p*-methylphenylamine, 106-49-0; *p*-methoxyphenylamine, 104-94-9; *p*-chlorophenylamine, 106-47-8; *p*-bromophenylamine, 106-40-1; *p*-nitrophenylamine, 100-01-6; *p*-(trifluoromethyl)phenylamine, 455-14-1.

Supplementary Material Available: Tables of thermal parameters and hydrogen atom parameters for Cu$_2$(PAAet)$_2$·$^1/_2C_6H_6$ and Cu$_2$(PAApr)$_2$ (6 pages); listings of observed and calculated structure factors for both compounds (48 pages). Ordering information is given on any current masthead page.

(46) Scheidt, W. R.; Kastner, M. E.; Hatano, K. *Inorg. Chem.* **1978**, *17*, 706. Scheidt, W. R.; Reed, C. A. *Inorg. Chem.* **1978**, *17*, 710.
(47) Schmitt, R. D.; Wing, R. M.; Maki, A. H. *J. Am. Chem. Soc.* **1969**, *91*, 4394.
(48) Guthrie, J. W.; Lintvedt, R. L.; Glick, M. D. *Inorg. Chem.* **1980**, *19*, 2949.
(49) See ref 14, 23-25, 43.

Contribution from the Institut für Anorganische Chemie, Technische Hochschule Darmstadt, D-6100 Darmstadt, West Germany, and Laboratoire de Chimie des Métaux de Transition et de Catalyse associé au CNRS, Université Louis Pasteur, F-67008 Strasbourg, France

Metal Complexes with Tetrapyrrole Ligands. 46.[1] Europium(III) Bis(octaethylporphyrinate), a Lanthanoid Porphyrin Sandwich with Porphyrin Rings in Different Oxidation States, and Dieuropium(III) Tris(octaethylporphyrinate)

Johann W. Buchler,*[2] André de Cian,[3] Jean Fischer,[3] Martina Kihn-Botulinski,[2] and Raymond Weiss*[3]

Received June 4, 1987

Reaction of tris(2,4-pentanedionato)europium(III) with octaethylporphyrin [H_2(OEP)] in refluxing 1,2,4-trichlorobenzene (TCB) produces a mixture of double-decker europium(III) bis(octaethylporphyrinate) [Eu(OEP)$_2$, **2**] and triple-decker dieuropium(III) tris(octaethylporphyrinate) [Eu$_2$(OEP)$_3$, **4**], which are separated by chromatography. **2** is characterized by UV/vis, near-IR, IR, ^{1}H NMR, ESR, and mass spectra. Crystals of **2** (monoclinic, $P2_1/n$) are isomorphous with those of the known cerium(IV) sandwich Ce(OEP)$_2$ (**1**). The presence of Eu^{III} follows from the temperature dependence of the magnetic moment. The well-defined composition Eu(OEP)$_2$ requires that one of the porphyrin rings is electron-deficient; i.e., the charge of the Eu^{III} ion is compensated for by the normal porphyrinate dianion and a porphyrinate monoanion radical. The presence of a porphyrin radical is deduced from near-IR, IR, and NMR data, but the hole cannot be assigned to a specific ring on the time scales available. In refluxing TCB, **2** is transformed into **4** and H_2(OEP). Reduction of **2** with sodium anthracenide furnishes the anion [Eu(OEP)$_2$]$^-$.

Since the first observation of octacoordination in bis(acetato)zirconium(IV) and -hafnium(IV) porphyrins,[4] interest in porphyrin complexes with coordination number 8 has gradually increased. The bis(β-diketonato) species M(P)(acac)$_2$[5] with M^{IV} = Zr,[6] Hf,[6] Th,[7-9] and U[8] are well-defined compounds. The crystal

(1) Part 45: Buchler, J. W.; Herget, G. *Z. Naturforsch., B: Anorg. Chem., Org. Chem.* **1987**, 42B, 1003-1008.
(2) Technische Hochschule Darmstadt.
(3) Université Louis Pasteur.
(4) (a) Buchler, J. W.; Eikelmann, G.; Puppe, L.; Rohbock, K.; Schneehage, H. H.; Weck, D. *Justus Liebigs Ann. Chem.* **1971**, *745*, 135-151. (b) Hoard, J. L. In *Porphyrins and Metalloporphyrins*; Smith, K. M., Ed.; Elsevier: Amsterdam, 1975; pp 317-380. (c) Buchler, J. W. *Angew. Chem.* **1978**, *90*, 425-442; *Angew. Chem., Int. Ed. Engl.* **1978**, *17*, 403-423.
(5) Abbreviations used: M, metal; (P)$^{2-}$, (OEP)$^{2-}$, (Pc)$^{2-}$, (TPP)$^{2-}$, (TTP)$^{2-}$, and (TAP)$^{2-}$, dianions of a general porphyrin, 2,3,7,8,12,13,17,18-octaethylporphyrin, phthalocyanine, 5,10,15,20-tetraphenylporphyrin, 5,10,15,20-tetra-*p*-tolylporphyrin, and 5,10,15,20-tetra-*p*-anisylporphyrin, respectively; Ln, lanthanoid metal; H(acac), acetylacetone; HOAc, acetic acid; TCB, 1,2,4-trichlorobenzene; TLC, thin-layer chromatography; near-IR, near-infrared.
(6) Buchler, J. W.; Folz, M.; Habets, H.; van Kaam, J.; Rohbock, K. *Chem. Ber.* **1976**, *109*, 1477-1485.

0020-1669/88/1327-0339$01.50/0

Table I. ^{1}H NMR Data (300 MHz) for Eu(OEP)$_2$ (**2**), Its Reduction Product Na[Eu(OEP)$_2$], and Eu$_2$(OEP)$_3$ (**4**), Together with Reference Data for Ce(OEP)$_2$ (**1**) and La$_2$(OEP)$_3$

compd	param	CH=(e)[b]	CH=(i)[c]	CH_2(i)	CH_2(e,1)[d]	CH_2(e,2)[d]	CH_3(i)	CH_3(e)
$Eu_2(OEP)_3$	δ[a]	12.77	13.59	5.57	5.14	2.80	4.75	0.34
	J,[e] Hz	s	s	q, 7.5	dq, 14	dq, 14	t, 7.5	t, 7.5
	δ_{iso}[f]	4.58	5.46	1.48	1.42	−0.57	2.16	−0.61
$La_2(OEP)_3$	δ	8.19	8.13	4.09	3.72	3.37	2.59	0.95
$Ce(OEP)_2$	δ	9.11			4.20	3.86		1.68
$Eu(OEP)_2$	δ	~22[g]			22.62	14.60		3.41
	$w_{1/2}$, Hz	>125			125	95		22
	δ_{iso}[h]	~13			18.76	10.40		1.73
	δ_{iso}(rad)[i]	~8			18.72[j]	10.53[j]		3.13
$[Eu(OEP)_2]^-$	δ	14.29	12.22	5.93	4.07	3.90	2.23	1.96
	J,[e] Hz	s	s	m	dq, 13	dq, 13	t, 6	t, 7
	δ_{iso}[f]	5.18	3.11	1.90[k]	0.04[j]	−0.13[j]	0.55	0.28

[a] Versus internal TMS. [b] Methine protons of external (e) ring. [c] Methine protons of internal (i) ring. [d] 1 and 2 denote exo and endo methylene protons, respectively (assignment arbitrary). [e] Letters indicate multiplicity of the resolved signal. [f] Isotropic shift $\delta_{iso} = \delta_{para}(Eu^{III}) - \delta_{dia}(La^{III})$. [g] Signal hidden under that for CH_2 (i). [h] Isotropic shift $\delta_{iso} = \delta_{para}(Eu^{III}) - \delta_{dia}(Ce^{IV})$. [i] Isotropic shift of the radical part, $\delta_{iso}(rad) = \delta_{iso}(Eu^{III}/rad) - \delta_{iso}(Eu^{III})$. [j] Reference is $^1/_2[\delta_{CH_2(e,1)} + \delta_{CH_2(e,2)}]$ because of ambiguity of assignment.

Chart I. Bar Graphs Illustrating the Configurations of the Double-Deckers M(P)$_2$ and Triple-Deckers M$_2$(P)$_3$ (P = OEP)

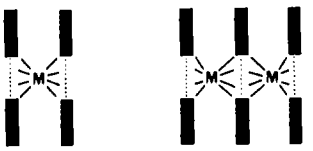

1: Ce(OEP)$_2$, M = Ce
2: Eu(OEP)$_2$, M = Eu
3: Ce$_2$(OEP)$_3$, M = Ce
4: Eu$_2$(OEP)$_3$, M = Eu

structure of Th(OEP)(acac)$_2$ has been described.[8] The shape of the molecule is derived from a square antiprism, as in Hf(OEP)(OAc)$_2$[4b]. Another series of octacoordinated metal tetrapyrroles are the actinoid sandwich systems An(Pc)$_2$ (An = Th, U)[10a] or U(TPP)$_2$[10b] or the lanthanoid double-deckers Ln(Pc)$_2$.[11] The latter compounds are intensively studied as prospective materials for electrical devices such as semiconductors or color displays.[12] Therefore, synthetic studies on these sandwich systems are under way at both Strasbourg (preferentially phthalocyanine systems)[13,14] and Darmstadt (porphyrin systems).[9,15-19] Crystal structures of lanthanoid tetrapyrroles have been reported for some monophthalocyaninates, namely Sm$_2$(Pc)(acac)$_4$[20] and Lu(Pc)(OAc)(H$_2$O)$_2$[13] and the double-deckers Nd(Pc)$_2$,[21] Lu(Pc)$_2$,[13] and Ce(OEP)$_2$[18] (**1**), as well as the triple-deckers Nd$_2$(Pc)$_2$(TAP)[14] and Ce$_2$(OEP)$_3$ (**3**).[18] The general configuration of these double- and triple-deckers, M(P)$_2$ and M$_2$(P)$_3$, respectively, is shown in Chart I.

This paper describes the synthesis, the structure, and some properties of the europium(III) bis(porphyrinate) Eu(OEP)$_2$ (**2**) and the characterization of the tris(porphyrinate) Eu$_2$(OEP)$_3$ (**4**).[22] Preliminary reports on this compound have already appeared,[16] along with various data on the similar compound Pr(OEP)$_2$[16] and the optical spectra of the whole series of compounds Ln(OEP)$_2$ (Ln = La–Lu apart from Pm).[9,17]

Experimental Section

Material and Methods. Chemicals and instruments used were the same as previously described[18] if not stated below. Eu(acac)$_3$·H$_2$O was prepared by following literature methods.[23] Near-infrared spectra were taken with a Zeiss DMR 21 spectrophotometer. The ESR spectra at various temperatures (Varian X-band, E-line spectrometer; 9.25 GHz; sample dissolved in deoxygenated toluene and sealed) and the magnetic susceptibility curve of Eu(OEP)$_2$ (2.6–300 K; vibrating-reed magnetometer[24]) were obtained by N. Preusse and D. Flasche at the Institut für Festkörperphysik, Technische Hochschule Darmstadt (courtesy of Professor B. Elschner). The magnetic susceptibility (298 K; Faraday balance[25]) of Eu$_2$(OEP)$_3$ was determined by Dr. H. Astheimer at the Institut für Physikalische Chemie, Technische Hochschule Darmstadt (courtesy of Professor W. Haase). A 0.25 M solution of sodium anthracenide in THF was prepared as described before.[26]

Synthesis of Bis(2,3,7,8,12,13,17,18-octaethylporphyrinato)europium(III), Eu(OEP)$_2$ (2), and Tris(2,3,7,8,12,13,17,18-octaethylporphyrinato)dieuropium(III), Eu$_2$(OEP)$_3$ (4). A solution of 300 mg (0.566 mmol) of H$_2$(OEP) and 1 g (1.98 mmol) of Eu(acac)$_3$·H$_2$O in 50 mL of TCB is refluxed under a slow stream of nitrogen ("reinst"/99.99%; O_2 < 50 ppm). The color of the initially red-violet reaction mixture changes to cherry-red after 4 h and to reddish brown after 20 h when the TCB is removed in a high vacuum at 50 °C. The blue-violet residue is chromatographed at an alumina column (grade I, basic, 3.5 × 7 cm) with toluene. After a small orange-yellow forerun consisting of Eu(OEP)(acac) and TCB, a yellow-brown fraction I is eluted. With toluene/methanol (100:1), a red-brown fraction II is obtained. Further elution with methanol removes some unreacted Eu(acac)$_3$. The column shows

(7) Wong, L. P.; Horrocks, W. D., Jr. *Tetrahedron Lett.* **1975**, 2637–2641.
(8) Dormond, A.; Belkalem, B.; Charpin, P.; Lance, M.; Vigner, D.; Folcher, G.; Guilard, R. *Inorg. Chem.* **1986**, *25*, 4785–4790.
(9) Kihn-Botulinski (formerly Knoff), M. Doctoral Dissertation, Technische Hochschule Darmstadt, 1986.
(10) Lux, F.; Dempf, D.; Graw, D. *Angew. Chem.* **1968**, *80*, 792; *Angew. Chem., Int. Ed. Engl.* **1968**, *7*, 819.
(11) For reviews, see (a) *Gmelins Handbuch der Anorganischen Chemie*, 8th ed.; Springer: West Berlin, 1980; Syst. No. 39, Rare Earth Elements, Part D1, pp 89–101. (b) Kasuga, K.; Tsutsui, M. *Coord. Chem. Rev.* **1980**, *32*, 67–95.
(12) (a) Corker, G. A.; Grant, B.; Clecak, N. J. *J. Electrochem. Soc.* **1979**, *126*, 1339–1343. (b) Collin, G. C. S.; Schiffrin, D. J. *J. Electroanal. Chem. Interfacial Electrochem.* **1982**, *139*, 335–369. (c) André, J. J.; Holczer, K.; Petit, P.; Riou, M. T.; Clarisse, C.; Even, R.; Fourmige, M.; Simon, J. *Chem. Phys. Lett.* **1985**, *115*, 463–466.
(13) De Cian, A.; Moussavi, M.; Fischer, J.; Weiss, R. *Inorg. Chem.* **1985**, *24*, 3162–3167.
(14) Moussavi, M.; De Cian, A.; Fischer, J.; Weiss, R. *Inorg. Chem.* **1986**, *25*, 2107–2108.
(15) Buchler, J. W.; Kapellmann, H. G.; Knoff, M.; Lay, K. L.; Pfeifer, S. *Z. Naturforsch.*; B: *Anorg. Chem., Org. Chem.* **1983**, *38B*, 1339–1345.
(16) Buchler, J. W.; Knoff, M. In *Optical Spectra and Structure of Tetrapyrroles*; Blauer, G., Sund, H., Eds.; de Gruyter: West Berlin 1985; pp 91–105.
(17) Buchler, J. W.; Elsässer, K.; Kihn-Botulinski, M.; Scharbert, B.; Tansil, S. *ACS Symp. Ser.* **1986**, *321*, 94–104.
(18) Buchler, J. W.; de Cian, A.; Fischer, J.; Kihn-Botulinski, M.; Paulus, R.; Weiss, R. *J. Am. Chem. Soc.* **1986**, *108*, 3652–3659.
(19) Buchler, J. W.; Elsässer, K.; Kihn-Botulinski, M.; Scharbert, B. *Angew. Chem.* **1986**, *98*, 257–258; *Angew. Chem., Int. Ed. Engl.* **1986**, *25*, 286–287.
(20) Sugimoto, H.; Higashi, T.; Maeda, A.; Mori, M.; Masuda, H.; Taga, T. *J. Chem. Soc., Chem. Commun.* **1983**, 1234–1235.
(21) (a) Kasuga, K.; Tsutsui, M.; Petterson, R. C.; Tatsumi, K.; van Opdenbosch, N.; Pepe, G.; Meyer, E. F., Jr. *J. Am. Chem. Soc.* **1980**, *102*, 4836–4838. (b) Darovskikh, A. N.; Tsytsenko, A. K.; Frank-Kamenetskaya, O. V.; Fundamenskii, V. S.; Moskalev, P. N. *Sov. Phys.—Crystallogr.* (*Engl. Transl.*) **1984**, *29*, 273–276.
(22) The element *Europium* is certainly inviting to a *Franco-German* collaboration.
(23) Stites, J. G.; McCarty, C. N.; Quill, L. L. *J. Am. Chem. Soc.* **1948**, *79*, 3142–3143.
(24) Unterreiner, K.-H. Doctoral Dissertation, Technische Hochschule Darmstdt, 1969.
(25) Merz, L. Doctoral Dissertation, Technische Hochschule Darmstadt, 1979.
(26) Buchler, J. W.; Puppe, L. *Justus Liebigs Ann. Chem.* **1970**, *740*, 142–163.

a pink color due to Eu(OEP)(acac), which is difficult to elute. After evaporation of the solvents and recrystallization from benzene/TCB (5:1), I consists of an insoluble gel and traces of **4** and II of a mixture of **2** and **4** that is separated by fractional crystallization. **4** is much less soluble in organic solvents than **2** and crystallizes first as small dark blue crystals of $Eu_2(OEP)_3 \cdot 2TCB$ (69 mg, 16%), followed by large, dark blue crystals of $Eu(OEP)_2$ (268 mg, 79%). Anal. Calcd for **4**, $C_{120}H_{138}N_{12}Cl_6Eu_2$ (mol wt 2265.13): C, 63.63; H, 6.14; N, 7.42; Cl, 9.39. Found: C, 63.84; H, 6.19; N, 7.37; Cl, 8.55. Calcd for **2**, $C_{72}H_{88}N_8Eu$ (mol wt 1217.52): C 71.03; H, 7.29; N, 9.20. Found: C, 70.85; H, 7.30; N, 9.09. Infrared spectra (KBr; only bands that are not common to both compounds are given): **4**, 1525, 1506, 835, 659 cm^{-1}; **2**, 831, 841 cm^{-1}. Mass spectra (field ion desorption mode): Only **2** gave a molecular ion; calcd for ^{153}Eu, M 1218.54; found, M 1217.5. UV/vis spectra [λ_{max}/nm (log ϵ)]: **4** (diethylene glycol–diethyl ether), 800 (3.03), 664 (3.32), 574 (3.74), 532 (3.75), 381 (5.27); **2** (cyclohexane), 676 (3.36), 543 (3.87), 376 (5.04), 340 (4.89, shoulder). Near-IR spectrum [λ_{max}/nm (log ϵ), cyclohexane]: **2**, 1280 (3.89). Lattice parameters[16] of $Eu_2(OEP)_3 \cdot 2TCB$: tetragonal body-centered, a = 14.77, c = 28.82 Å, V = 6290 Å^3. For NMR spectra of **2** (in toluene-d_8) and **4** (in CCl_4), see Table I.

Formation of the Triple-Decker Compound $Eu_2(OEP)_3$ (4) from the Double-Decker Compound Eu(OEP)$_2$ (2) ("Raise by One Story Reaction"). A 100-mg (0.082-mmol) sample of $Eu(OEP)_2$ (**2**) (dried at 50 °C for 3 d) was heated in 50 mL of boiling, dry TCB under Ar for 20 h. After the TCB was removed in a high vacuum, the dark blue residue was chromatographed with toluene on an alumina column (grade I, basic, 3.5 × 7 cm). After evaporation of the solvent in vacuo, the first dark blue fraction yielded after recrystallization from benzene/TCB (5:1) 44.5 mg (0.023 mmol, 57%) $Eu_2(OEP)_3 \cdot 2TCB$ as small dark blue, sparingly soluble crystals. A second, reddish brown fraction was eluted with toluene and consisted of unreacted **2**. A third red-brown, strongly fluorescing fraction was obtained with chloroform and contained octaethylporphyrin [H_2(OEP)] and traces of unknown decomposition products. This fraction was rechromatographed with chloroform on an alumina column (grade Super I, neutral, 3.5 × 20 cm). The red main fraction was freed from the solvent in vacuo, the residue suspended in methanol (in which H_2(OEP) is insoluble) and filtered, and the contents of the filter weighed (12.5 mg, 0.023 mmol of H_2(OEP). Thus, **4** and H_2(OEP) are formed in a 1:1 molar ratio.

Sodium Bis(2,3,7,8,12,13,17,18-octaethylporphyrinato)europate(III) in Tetrahydrofuran. A solution of 5 mg (0.004 mmol) of $Eu(OEP)_2$ (dried in vacuo at 50 °C) in 0.5 mL of toluene-d_8 containing a trace of TMS was placed under Ar into a dry NMR tube and sealed with a septum cap and Nescoe film. With a Hamilton sypringe, 15 μL of 0.25 M sodium anthracenide in THF was added and a ^1H NMR spectrum taken (see Table I); apart from the signals of $[Eu(OEP)_2]^-$, stronger signals of THF and weaker signals of anthracene, toluene, TMS, and H_2(OEP) were noted. Afterward, the red-brown solution was transferred (under air) to a cuvette for absorption spectroscopy. It did not show any absorption in the near-infrared region (900–200 nm). After evaporation of the solvents, a TLC analysis (neutral alumina, toluene) of the residue showed the presence of $Eu(OEP)_2$ and H_2(OEP) in about equal amounts.

X-ray Crystallography of Eu(OEP)$_2$. Crystals of **2** suitable for X-ray diffraction were obtained by slow evaporation of a n-decane solution. Diffraction data were collected at −100 °C on a Philips PW1100/16 automated diffractometer. Crystal data and data collection parameters are given as follows: formula, $C_{72}H_{88}N_8Eu$; mol wt 1217.52; crystal system, monoclinic; a = 15.392 (6), b = 15.279 (6), and c = 26.220 (8) Å; β = 89.89 (2) deg; V = 6166.3 Å^3; Z = 4; d (calcd) = 1.311 g/cm^3; μ = 10.645 cm^{-1}; space group, $P2_1/n$; radiation, graphite-monochromated Mo Kα; crystal size, 0.34 × 0.20 × 0.14 mm; scan mode, flying step scan, θ–2θ; $\Delta\theta = 0.9 + 0.346 (\tan\theta)°$; step width, 0.05 deg; scan speed, 0.024 deg/s; θ limits, 3/27 deg; octants, $\pm h,k,l$; number of measured data, 14 317; number of observed data, 8076 [rejection criterion, $I > 3\sigma(I)$]; absorbance minimum/maximum, 0.87/1.06; $R1 = \sum||F_o| - |F_c||/\sum|F_o| = 0.036$; $R2 = [\sum w(|F_o| - |F_c|)^2/\sum wF_o^2]^{-1/2} = 0.058$; $R_{fit} = [\sum w(|F_o| - |F_c|)^2/(N_{observns} - N_{params})]^{1/2} = 1.12$. The solution of the structure was taken from that of the isomorphous $Ce(OEP)_2$.[18] The determination of the elementary cell, check for stability of the crystal (no decomposition observed), raw step-scan data conversion to intensities, polarization and absorption corrections, inclusion of hydrogen atoms by their computed coordinates (C–H = 0.95 Å) and full-matrix least-squares refinement were performed as described for $Ce(OEP)_2$.[18]

Results and Discussion

(a) Chemistry. The formation of $Ln(OEP)_2$ double-deckers and $Ln_2(OEP)_3$ triple-deckers has been discussed before.[16-18] Prolonged boiling of $Ln(acac)_3$ and H_2(OEP) in trichlorobenzene and the presence of some oxidant is necessary. A secondary intermediate—not observed with Eu^{III}—is the lanthanoid hydrogen bis(porphyrinate), $LnH(OEP)_2$, which either reacts with the primary intermediate Ln(OEP)(acac) in a condensation reaction to produce the triple-decker $Ln_2(OEP)_3$ or is dehydrogenated to the symmetrical double-decker $Ln(OEP)_2$. $Eu(OEP)_2$ (**2**) and $Eu_2(OEP)_3$ (**4**) both closely resemble their cerium analogue: **2** is rather soluble even in alkanes, while **4** is practically insoluble in most solvents like dichloromethane and toluene. The "raise by one story reaction" (1) observed with $Ce(OEP)_2$ (**1**)[18] has been

$$2Eu(OEP)_2 + 2H^+ + 2e^- \rightarrow Eu_2(OEP)_3 + H_2(OEP) \quad (1)$$

realized in a preparative scale with **2**. The nature of the required reducing agent has not become clear. It is assumed that initially a double-decker monoanion is formed that is partially demetalated by traces of residual water and acid according to (1a). The resulting europium(III) monoporphyrin then reacts with another double-decker monoanion to yield the triple-decker by (1b). The

$$[Eu(OEP)_2]^- + H_3O^+ \rightarrow Eu(OEP)OH + H_2(OEP) \quad (1a)$$

$$[Eu(OEP)_2]^- + Eu(OEP)OH \rightarrow Eu_2(OEP)_3 + OH^- \quad (1b)$$

reduction of **2** to its monoanion was done on purpose with sodium anthracenide (Na[Anthr]) according to (2) in THF. The dou-

$$Eu(OEP)_2 + Na[Anthr] \rightarrow Na[Eu(OEP)_2] + Anthr \quad (2)$$

ble-decker anion $[Eu(OEP)_2]^-$ is unstable in moist air and slowly reverts to **2**, presumably via $EuH(OEP)_2$, which is also partially demetalated.

(b) Identification. $Eu(OEP)_2$ (**2**) and $Eu_2(OEP)_3$ (**4**) are identified by elemental analyses, their TLC R_f values (**2**, 0.55, in toluene; **4**, 0.42, in tetrachloromethane), infrared spectra showing all the typical bands of octaethylporphyrin complexes lacking axial ligands, magnetic measurements, and optical spectra.[16,17] Only **2** gave a molecular ion in the mass spectrum.

$Eu_2(OEP)_3$ (**4**) is a very close analogue of $Ce_2(OEP)_3$ (**3**). The magnetic moment at room temperature is 3.17 μ_B/Eu^{III}; expected is 3.5 μ_B.[27] There is no problem with the valency of the lanthanoid central ions. The ^1H NMR spectrum clearly shows the resonances of the two external rings and the internal porphyrin ring in the expected 2:1 intensity ratio (for data, see Table I; the assignments given have been checked by selective decoupling in double-resonance experiments). The diamagnetic compound $La_2(OEP)_3$ serves as a reference for the noted isotropic shifts $\delta_{iso} = \delta_{para} - \delta_{dia}$.[28] Apart from the methyl and half of the methylene resonances of the external rings, all isotropic shifts are positive, indicating low-field shifts; their sign and order of magnitude are expected for Eu^{III} complexes.[29] Plausibly, the isotropic shifts of the internal ring are larger than those of the external ring, because the internal ring is influenced by two connective Eu^{III} ions while the external rings only feel one of those. The data are consistent with a composition $\langle 2Eu^{3+}/3(OEP)^{2-}\rangle$ for $Eu_2(OEP)_3$.

As regards **2**, the formula $Eu(OEP)_2$ is corroborated by the mass spectrum and the crystallographic data (see below). As we dispose of the hydrogen lanthanoid(III) bis(porphyrinates) in the case of $PrH(OEP)_2$[19] and $PrH(TTP)_2$,[15] we know that they can be discerned by their IR, near-IR, and mass spectra from $Pr(OEP)_2$[9] and $Pr(TPP)_2$,[17] respectively. Therefore, we are certainly not dealing with $EuH(OEP)_2$. The formula $Eu(OEP)_2$ however may be represented by three compositions:

$$\underset{\mathbf{2a}}{\langle Eu^{2+}/2(OEP^{\bullet})^-\rangle} \quad \underset{\mathbf{2b}}{\langle Eu^{3+}/(OEP)^{2-}/(OEP^{\bullet})^-\rangle}$$

$$\underset{\mathbf{2c}}{\langle Eu^{4+}/2(OEP)^{2-}\rangle}$$

2a contains an Eu^{II} ion combined with two electron-deficient

(27) Weiss, A.; Witte, H. *Magnetochemie*; Verlag *Chemie*: Weinheim, FRG, 1973.
(28) Horrocks, W. D., Jr. In *NMR of Paramagnetic Molecules; Principles and Application*, in La Mar, G. N., Horrocks, Jr., W. D., Jr., Holm, R. H., Eds., Academic: New York, 1973; pp 479–519.
(29) Horrocks, W. D., Jr.; Sipe, J. P., III. *J. Am. Chem. Soc.* **1973**, *93*, 6800–6804.

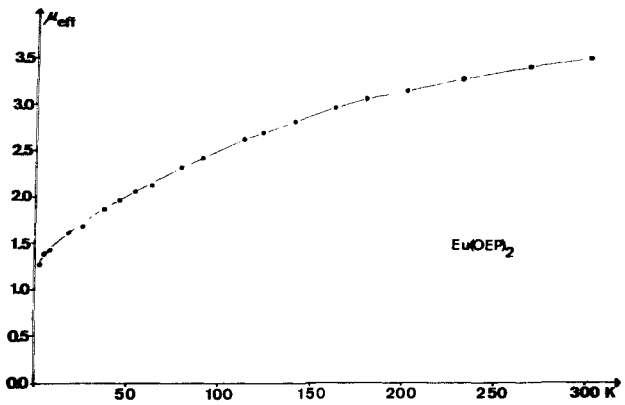

Figure 1. Temperature dependence of the magnetic moment μ_{eff} of $Eu(OEP)_2$ (**2**). (Values calculated from $\mu_{eff} = 2.83(\chi_{met}T)^{1/2}$ (μ_B). χ_{met} values are given in Table V. $\chi_{met} = \chi_{mol} - \chi_{dia}$; $\chi_{dia} = -960 \times 10^{-6}$ cm^3 mol^{-1}, as calculated for two OEP systems.)

porphyrin monoanion radicals, **2b** an Eu^{III} ion with a normal porphyrinate dianion and an electron-deficient porphyrin monoanion radical, and **2c** an Eu^{IV} ion with two normal porphyrinate dianions. The magnetic data allow us to take **2b** as the realistic choice: the magnetic moment of **2** is 3.55 μ_B at 302 K, and falls to 1.28 μ_B at 2.6 K (see Figure 1). For **2a**, a high moment of at least 7.9 μ_B due to Eu^{II} and an additional contribution of the two radical spins would be expected although the latter may be canceled by spin-pairing of the cofacial radical systems as observed with the π-radical dimer $[Zn(OEP)Br]_2$.[30] **2c** would contain the hitherto unknown Eu^{IV}. This is isoelectronic with Sm^{III}, which usually has a rather small moment of 1.55–1.65 μ_B. The observed moment is at 300 K clearly inbetween and distinctly different from the values expected for **2a** and **2c**.

For Eu^{III} alone, 3.51 μ_B would be expected. The additional porphyrin radical spin with its spin-only value would combine with the moment of Eu^{III} affording $\mu_{eff} = [\mu^2(Eu) + \mu^2(OEP)]^{1/2} =$ 3.9 μ_B. The observed value is close to this value. Furthermore, the temperature dependence of μ_{eff} is reminiscent of the typical curve for Eu^{III} alone, for which, close to 0 K, the moment vanishes. For **2**, the moment drops to 1.28 μ_B (see Figure 1), a value that may represent the residual paramagnetism caused by the porphyrin π-radical.

The typical magnetism of Eu^{III} may also explain the temperature dependence of an exploratory ESR spectrum of **2** (Figure 2). At 200 K in toluene solution, there is a broad line typical for an organic radical ($g = 2.0$), and it is not surprising that some fine structure emerges on cooling and freezing the solution. The best resolution is seen at 58 K. At present, we cannot explain the fine structure of this spectrum, which certainly will be complicated by interference of the electron spins of the porphyrin π-radical and Eu^{III} and the nuclear spins of ^{151}Eu and ^{153}Eu, apart from ^{14}N and ^{1}H couplings. On further cooling, the fine structure disappears again. This could be due to the fact that the paramagnetism of Eu^{III} vanishes at 20 K and hence does not contribute to the fine structure any more.

The ^1H NMR spectrum of $Eu(OEP)_2$ (**2**: data in Table I) is very much different in type from the spectrum of **4**. This is seen in the chemical shifts and the line widths of the signals. There are just three broad peaks at 3.41, 14.60, and 22.62 ppm.[16] The assignments indicated in the table are based on integrated intensity ratios, which disclose that the methine signal must be hidden under the methylene signal at 22.62 ppm. The multiplicity of the signals indicates only one set of methyl and two sets of diastereotopic methylene protons. The same situation was observed with **1**.[18] On the NMR time scale, therefore, the two porphyrin rings are identical, and the π-electron hole seems to be delocalized. One could argue that, with a localized hole, the radical part of the NMR spectrum would be very broad and that only the spectrum

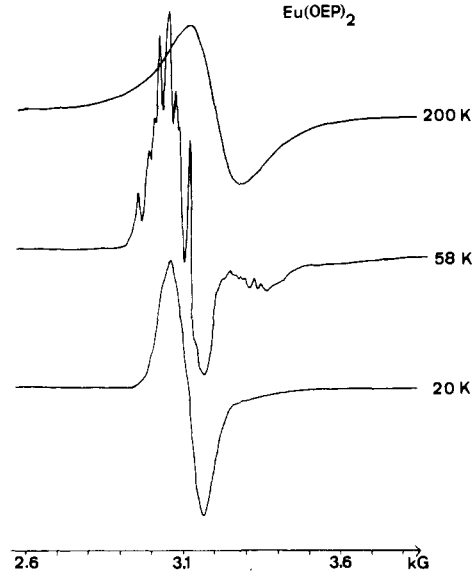

Figure 2. Electron spin resonance spectra of $Eu(OEP)_2$ (**2**) (taken in toluene at the temperatures indicated; see Experimental Section and text).

of the electronically saturated porphyrin ring is observed. However, the line width of the NMR spectra of organic radicals is reduced in the presence of other paramagnetic molecules acting as "spin relaxers".[31] Here, Eu^{III} would be the spin relaxer allowing us to observe the π-radical spectrum at a reasonable line width.

The isotropic shifts of **2** using **1** as a diamagnetic reference are unusually large for a pure Eu^{III} species. This becomes obvious on comparison with the data of **4**. If composition **2b** applies, the observed shift δ_{iso} should be the sum of two components:

$$\delta_{iso} = \delta_{iso}(Eu^{III}) + \delta_{iso}(rad)$$

where $\delta_{iso}(Eu^{III})$ is the contribution of the Eu^{III} ion and $\delta_{iso}(rad)$ the contribution of the electron-deficient porphyrin π-radical if these contributions were just additive. Anyway, it seems reasonable to ascribe the large shifts observed with **2** to an influence of the π-radical. This argument is reinforced by the NMR data of the anion $[Eu(OEP)_2]^-$ (see Table I) prepared from **2** according to (2). They show isotropic shifts that are solely due to Eu^{III} and have the same order of magnitude as the signals of the triple-decker **4**. The shifts of the double-decker anion may then be used to calculate the radical contribution, $\delta_{iso}(rad)$, shown in Table I.

The infrared spectra of $Eu(OEP)_2$ (**2**) have extra bands that are absent in all the other compounds listed in Table I. They occur at 1525 and 1506 cm^{-1} and as a broad background between 1200 and 1350 cm^{-1}. Zinc, iron, and cobalt complexes containing uninegative octaethylporphyrin π-radicals as equatorial ligands typically have distinct extra bands between 1500 and 1550 cm^{-1} ("oxidation state markers").[32]

Striking differences are seen in the optical absorption spectra of $Eu(OEP)_2$ and $Ce(OEP)_2$ presented in Figure 3. While the visible spectrum of the Ce^{IV} sandwich **1** has a "normal" appearance[33] with an additional tail extending into the near-IR region, which may be ascribed to exciton interactions,[16,17] the spectrum of the Eu^{III} sandwich **2** does not have the pronounced $Q(0,0)$ band at 573 nm but rather a washed-out spectrum with features at 540 and 670 nm that are typical for π-radicals formed, e.g., by one-electron oxidation from Zn(OEP).[30] More interesting is the near-infrared region. **2** has a strong band at 1280 nm with a molar extinction coefficient of 7800. This is absent in all the other species shown in table I, especially in the one-electron-re-

(30) Fuhrhop, J. H.; Wasser, P.; Riesner, D.; Mauzerall, D. *J. Am. Chem. Soc.* **1972**, *94*, 7996–8001.

(31) Yamauchi, F.; Kreilick, R. W. *J. Am. Chem. Soc.* **1969**, *91*, 3429–3432.

(32) Shimomura, E. T.; Philipi, M. A.; Goff, H. M.; Scholz, W. F.; Reed, C. A. *J. Am. Chem. Soc.* **1981**, *103*, 6778–6780.

(33) Gouterman, M. In *The Porphyrins*; Dolphin, D., Ed.; Academic: New York, 1978; Vol. 3, pp 1–165.

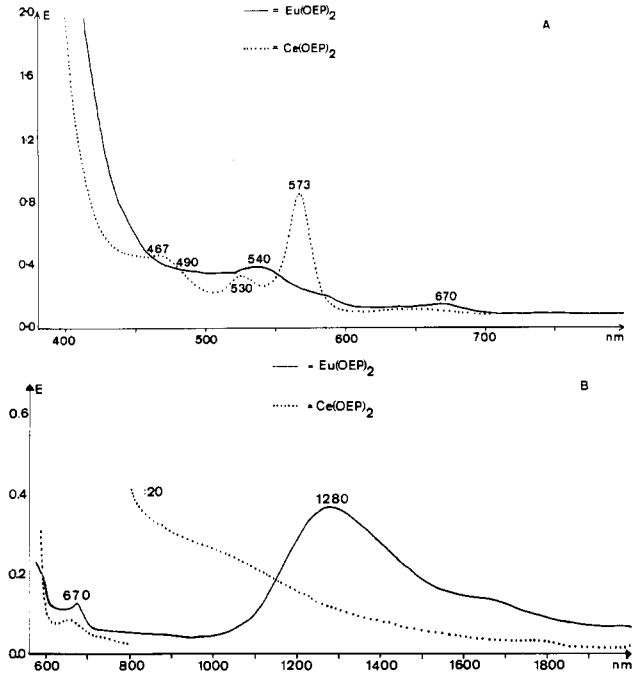

Figure 3. Optical absorption spectra of $Eu(OEP)_2$ (**2**) and $Ce(OEP)_2$ (**1**):(A) UV/vis range; (B) near-IR range (for extinction coefficients, see Experimental Section).

duction product of **2**. Furthermore, near-IR bands are unknown for monoporphyrin π-radicals but do occur when they dimerize at low temperatures and high concentrations.[30] Therefore, this band must be a property of the electron-deficient sandwich system.

We suggest that the NIR band of **2** is an internal charge-transfer (CTI) band, visualizing that compounds like **2** with the composition **2b** are internal electron-donor–acceptor (EDA or CT) complexes in which the porphyrin dianion acts as the donor and the porphyrin monoanion radical supplies the acceptor.[34] High extinction coefficients are reasonable because the donor and acceptor species are firmly attached to each other by the Eu^{III} ion. Another attractive view explained elsewhere[17] is the idea that sandwich systems like $Eu(OEP)_2$ represent "inverse mixed-valence" complexes. Normal "mixed-valence" complexes consist of two metal ions in different oxidation states bridged by a common ligand. In this case, two ligands in different oxidation states are bridged by a common metal ion.

This CTI band has been detected in all the octaethylporphyrinate sandwiches containing trivalent central ions, namely $Ln(OEP)_2$, where Ln = La and Pr–Lu save Pm,[16,17] and $Y(OEP)_2$.[35] Including the latter compound, the energy of the CTI band decreases as the ionic radius of the trivalent metal ion increases. Therefore, an involvement of f electrons in this kind of band can be excluded, and some steric effect of the two porphyrin systems (distance, distortions?) must be invoked. While on reduction of the uncharged Ln^{III} sandwiches the near-IR absorption vanishes, it appears when neutral Ce^{IV} double-deckers are oxidized. Thus, the radical cation $[Ce(OEP)_2]^+$ absorbs at 1270 nm.[19]

The cofacial array of two tetrapyrrole ligands in different oxidation states also occurs in the lanthanoid(III) bis(phthalocyaninates) $Ln(Pc)_2$, e.g. $Lu(Pc)_2$.[13] The near-IR spectra (700–1800 nm) of these comounds also show CTI bands.[36]

(c) Crystal Structure of $Eu(OEP)_2$ (2). In the crystalline state, **2** is isomorphous with $Ce(OEP)_2$[18] and consists of discrete $Eu(OEP)_2$ sandwich molecules linked solely by van der Waals contacts; there are no unusually short intermolecular contacts.

(34) Briegleb, G. *Elektronen-Donator-Akzeptor-Komplexe*; Springer: West Berlin, 1961.
(35) Buchler, J. W.; Hüttermann, J.; Löffler, J. *Bull. Chem. Soc. Jpn.* **1988**, *61*, 71–77.
(36) Markovitsi, D.; Thu, H. T. T.; Even, R.; Simon, J. *Chem. Phys. Lett.* **1987**, *137*, 107–112.

Table II. Mean Values of Selected Bond Lengths (Å), Bond Angles for (deg), and Individual Values of the Eu–N Bond Distances (Å) with Their Standard Deviations for $Eu(OEP)_2$ (**2**)

Bond Lengths					
	ring "N1"[a]		ring "N41"[a]		both rings
Eu–N[b]	Eu–N1	2.556 (4)	Eu–N41	2.513 (4)	
	Eu–N11	2.516 (4)	Eu–N51	2.493 (4)	
	Eu–N17	2.473 (4)	Eu–N57	2.491 (4)	
	Eu–N23	2.511 (4)	Eu–N63	2.527 (4)	
Eu–N		2.514		2.506	2.510
Bond Lengths for Skeleton Atoms[c]					
$N–C_\alpha$	1.368 (1)		$C_\alpha–C_m$	1.392 (2)	
$C_\alpha–C_\beta$	1.457 (2)		$C_\beta–C_\alpha$(Et)	1.496 (2)	
$C_\beta–C_\beta$	1.359 (3)		C_α(Et)–C_β(Et)	1.513 (3)	
Bond Angles[c]					
$C_\alpha–N–C_\alpha$	106.1 (1)		$C_\alpha–C_m–C_\alpha$	127.6 (1)	
$N–C_\alpha–C_\beta$	111.3 (1)		$N–C_\alpha–C_m$	124.0 (1)	
$C_\alpha–C_\beta–C_\beta$	106.5 (1)		$C_\beta–C_\alpha–C_m$	124.4 (1)	

[a] The porphyrin rings are specified by their nitrogen atom with the lowest count, i.e., "N1" or "N41"; see Figure 5a,b. [b] The numbering of the N atoms is given in Figure 5a,b. [c] C_α, C_β, C_m, C_α(Et), and C_β(Et) denote the α and β carbon atoms of the pyrrole ring, the methine carbon atom, and the two carbon atoms of the ethyl groups, respectively.

Table III. Additional Geometrical Parameters for $Eu(OEP)_2$ (**2**) Compared to Those of $Ce(OEP)_2$ (**1**) and $Ce_2(OEP)_3$ (**3**)

param		Eu-$(OEP)_2$	Ce-$(OEP)_2$	Ce_2-$(OEP)_3$
Orientation of the Macrocycles (deg)				
N1–Ct1–Ct2–N41[a]		43.1	41.8	24.5
Distances of the Mean Planes (Å)				
D_1, Ln–$(N_p)_4$[b]	N1···N23	1.433 (3)	1.375	1.394
	N41–N63	1.415 (3)	1.377	1.876
D_2, $(N_p)_4$–$(N_p)_4$	"N1"–"N41"	2.848	2.752	3.27
D_3, Ln–$C_{20}N_4$[c]	N1···N23	1.701 (3)	1.748	
	N41–N63	1.724 (3)	1.716	
D_4, $C_{20}N_4$–$C_{20}N_4$	"N1"–"N41"	3.425	3.464	3.54
D_5, $D_4 - D_2$		0.577	0.712	0.27
Inclination of the Mean Planes (deg)				
$(N_p)_4$	"N1"–"N41"	0.4	0.5	1.1
$C_{20}N_4$	"N1"–"N41"	1.4		
Inclination of the Pyrrole Rings[d] (deg)				
porphyrin ring "N1"		8.0	14.8	13.2
		11.3	11.7	13.8
		14.4	17.7	14.8
		16.5	15.4	15.7
porphyrin ring "N41"		8.4	13.2	2.3
		9.7	19.0	5.9
		13.9	14.3	0
		15.8	17.6	0
av		12.2	15.5	11.0
Ionic Radius of the Ln Ion (pm)[e]		107	97	114

[a] Angle of rotation of the porphyrin rings from the eclipsed position. Ct1 and Ct2 are the centroids of the N_4 mean planes of porphyrin rings "N1" and "N41". The mean values of the four possible angles are given. [b] $(N_p)_4$ denotes the mean plane of the four N atoms of a porphyrin ring. [c] $C_{20}N_4$ denotes the mean plane of the $C_{20}N_4$ core of the porphyrin ring ("core atoms"). [d] The dihedral angles of the mean planes of the pyrrole rings with the corresponding $(N_p)_4$ planes are given. The pyrrole rings are grouped according their porphyrin rings. [e] Ionic radii for coordination number 8 taken from Shannon and Prewitt.

Table II displays the essential bond lengths and angles; Table III gives additional geometrical data for comparison with data for $Ce(OEP)_2$ (**1**) and $Ce_2(OEP)_3$ (**3**). Figure 4 shows a stereoview of a single $Eu(OEP)_2$ molecule, Figure 5 gives the projections of the lower and upper halves of **2** and of the two superimposed macrocycles. The Eu^{III} ion is octacoordinate; the eight porphyrin N atoms form a nearly square antiprism. The configurations of **2** and **1** are identical, and at first glance, the conformations are

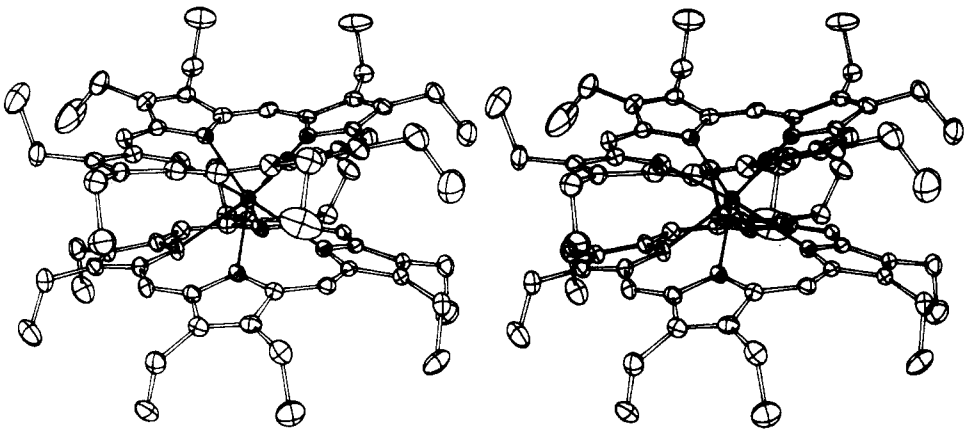

Figure 4. Stereoview generated from an ORTEP plot of a single $Eu(OEP)_2$ molecule as it exists in the crystal of **2**. Vibrational ellipsoids are drawn at the 50% probability level. Hydrogen atoms are omitted.

Table IV. Positional Parameters and Their Estimated Standard Deviations

atom	*x*	*y*	*z*	*B*,[a] Å^2	atom	*x*	*y*	*z*	*B*,[a] Å^2
Eu	0.00300 (2)	0.21995 (2)	0.24199 (1)	1.522 (4)	N41	−0.0096 (3)	0.3660 (3)	0.1985 (2)	1.99 (9)
N1	−0.0879 (3)	0.1764 (3)	0.1645 (2)	2.01 (9)	C42	−0.0605 (4)	0.4327 (4)	0.2163 (2)	2.3 (1)
C2	−0.1519 (3)	0.2303 (4)	0.1447 (2)	1.8 (1)	C43	−0.0963 (3)	0.4824 (4)	0.1744 (2)	1.9 (1)
C3	−0.1560 (3)	0.2205 (4)	0.0898 (2)	2.0 (1)	C44	−0.0610 (4)	0.4486 (4)	0.1306 (2)	2.1 (1)
C4	−0.0977 (3)	0.1564 (4)	0.0773 (2)	2.0 (1)	C45	−0.0057 (3)	0.3756 (4)	0.1464 (2)	2.0 (1)
C5	−0.0564 (4)	0.1297 (4)	0.1242 (2)	2.1 (1)	C46	0.0487 (4)	0.3293 (4)	0.1145 (2)	2.2 (1)
C6	0.0043 (4)	0.0618 (4)	0.1284 (2)	2.2 (1)	C47	0.1102 (3)	0.2657 (3)	0.1278 (2)	1.8 (1)
C7	0.0385 (3)	0.0279 (4)	0.1733 (2)	1.9 (1)	C48	0.1806 (4)	0.2365 (4)	0.0948 (2)	2.1 (1)
C8	0.0919 (4)	−0.0516 (4)	0.1762 (2)	2.0 (1)	C49	0.2312 (3)	0.1823 (4)	0.1234 (2)	2.0 (1)
C9	0.1066 (3)	−0.0668 (3)	0.2260 (2)	1.8 (1)	C50	0.1919 (3)	0.1798 (4)	0.1738 (2)	1.9 (1)
C10	0.0624 (3)	0.0028 (4)	0.2546 (2)	1.61 (9)	N51	0.1186 (3)	0.2300 (3)	0.1755 (2)	1.64 (8)
N11	0.0237 (3)	0.0604 (3)	0.2215 (2)	1.88 (9)	C52	0.2315 (3)	0.1409 (3)	0.2153 (2)	1.9 (1)
C12	0.0549 (3)	0.0068 (4)	0.3068 (2)	1.7 (1)	C53	0.2136 (3)	0.1543 (3)	0.2667 (2)	1.8 (1)
C13	0.0037 (3)	0.0633 (3)	0.3363 (2)	1.55 (9)	C54	0.2709 (3)	0.1283 (4)	0.3091 (2)	1.9 (1)
C14	−0.0141 (3)	0.0519 (4)	0.3897 (2)	1.7 (1)	C55	0.2371 (3)	0.1642 (4)	0.3519 (2)	2.0 (1)
C15	−0.0718 (3)	0.1157 (4)	0.4033 (2)	1.7 (1)	C56	0.1597 (3)	0.2123 (4)	0.3361 (2)	1.76 (9)
C16	−0.0882 (3)	0.1662 (3)	0.3572 (2)	1.51 (9)	N57	0.1461 (3)	0.2032 (3)	0.2851 (2)	1.61 (8)
N17	−0.0402 (3)	0.1340 (3)	0.3178 (2)	1.61 (8)	C58	0.1132 (3)	0.2678 (4)	0.3683 (2)	1.9 (1)
C18	−0.1519 (3)	0.2313 (3)	0.3528 (2)	1.7 (1)	C59	0.0519 (3)	0.3298 (4)	0.3549 (2)	1.9 (1)
C19	−0.1866 (3)	0.2663 (3)	0.3082 (2)	1.46 (9)	C60	0.0194 (4)	0.3988 (4)	0.3891 (2)	2.2 (1)
C20	−0.2678 (3)	0.3150 (4)	0.3054 (2)	1.8 (1)	C61	−0.0320 (4)	0.4513 (4)	0.3606 (2)	2.4 (1)
C21	−0.2860 (3)	0.3235 (4)	0.2552 (2)	1.9 (1)	C62	−0.0301 (4)	0.4153 (4)	0.3089 (2)	2.0 (1)
C22	−0.2144 (3)	0.2842 (4)	0.2275 (2)	1.73 (9)	N63	0.0190 (3)	0.3408 (3)	0.3071 (2)	1.72 (8)
N23	−0.1542 (3)	0.2510 (3)	0.2603 (2)	1.60 (8)	C64	−0.0712 (4)	0.4540 (4)	0.2678 (2)	2.0 (1)
C24	−0.2094 (3)	0.2793 (4)	0.1740 (2)	1.87 (9)	C65	−0.1553 (4)	0.5590 (4)	0.1792 (2)	2.7 (1)
C25	−0.2133 (4)	0.2719 (4)	0.0551 (2)	2.5 (1)	C66	−0.2464 (4)	0.5342 (5)	0.1965 (3)	3.7 (1)
C26	−0.2983 (4)	0.2287 (5)	0.0422 (3)	3.8 (1)	C67	−0.0728 (4)	0.4799 (4)	0.0770 (2)	2.6 (1)
C27	−0.0800 (4)	0.1174 (4)	0.0260 (2)	2.7 (1)	C68	−0.0093 (5)	0.5530 (5)	0.0631 (3)	4.1 (2)
C28	−0.1259 (5)	0.0302 (5)	0.0189 (3)	3.8 (2)	C69	0.1967 (4)	0.2685 (5)	0.0415 (2)	3.1 (1)
C29	0.1231 (4)	−0.1038 (4)	0.1314 (2)	2.3 (1)	C70	0.1494 (9)	0.2194 (7)	0.0012 (3)	9.4 (3)
C30	0.2091 (4)	−0.0703 (4)	0.1108 (2)	2.9 (1)	C71	0.3171 (4)	0.1446 (4)	0.1085 (2)	2.7 (1)
C31	0.1596 (4)	−0.1379 (4)	0.2497 (2)	2.4 (1)	C72	0.3911 (4)	0.2070 (5)	0.1199 (3)	4.3 (2)
C32	0.2471 (4)	−0.1071 (4)	0.2692 (3)	3.1 (1)	C73	0.3562 (4)	0.0810 (4)	0.3026 (2)	2.3 (1)
C33	0.0185 (4)	−0.0217 (4)	0.4230 (2)	2.4 (1)	C74	0.4306 (4)	0.1440 (5)	0.2920 (3)	4.5 (2)
C34	−0.0395 (5)	−0.1012 (5)	0.4222 (3)	3.5 (1)	C75	0.2740 (4)	0.1591 (4)	0.4044 (2)	2.6 (1)
C35	−0.1190 (4)	0.1258 (4)	0.4530 (2)	2.3 (1)	C76	0.2357 (5)	0.0854 (5)	0.4351 (3)	4.5 (2)
C36	−0.2067 (4)	0.0805 (5)	0.4521 (2)	3.4 (1)	C77	0.0426 (4)	0.4071 (4)	0.441 (2)	3.1 (1)
C37	−0.3210 (4)	0.3464 (4)	0.3497 (2)	2.4 (1)	C78	−0.0108 (6)	0.3490 (6)	0.4772 (3)	5.1 (2)
C38	−0.4003 (4)	0.2924 (5)	0.3612 (3)	3.4 (1)	C79	−0.0796 (4)	0.5323 (4)	0.3753 (2)	2.8 (1)
C39	−0.3680 (4)	0.3568 (4)	0.2311 (2)	2.3 (1)	C80	−0.1776 (5)	0.5168 (5)	0.3792 (3)	4.9 (2)
C40	−0.4259 (4)	0.2814 (5)	0.2138 (3)	3.3 (1)					

[a] Values for anisotropically refined atoms are given in the form of the isotropic equivalent thermal parameter defined as $^4/_3[a^2B(1,1) + b^2B(2,2) + c^2B(3,3) + ab(\cos\delta)V(1,2) + ac(\cos\beta)B(1,3) + bc(\cos\alpha)B(2,3)]$.

also practically identical. A minute difference is found in the orientation of the ethyl group containing C25 and C26 (Figure 5A). It is "exo" in **2**, "endo" in **1**. The bond distances and angles within the macrocycles do not significantly differ from each other in **2** and **1**.

Nevertheless, there are small, but important, differences in the bond lengths of the Ln–N bonds in the known double- and triple-deckers **1–3** that average to Eu–N = 2.510 Å (Table II), Ce^{IV}–N = 2.475 Å, and Ce^{III}–N = 2.63 Å.[18] The increase in Ln–N in the series $Ce^{IV} < Eu^{III} < Ce^{III}$ reflects an increase in the ionic radii: 97 < 107 < 114 pm (see Table III). Thus, the structural data confirm the assignment of the oxidation state +3 to the europium ion in **2**.

In the double- and triple-deckers **1–3**, the larger Ln ion effects an increase in the distances of the mean planes defined by the N atoms or the core atoms of the macrocycles. The difference D_5 between the two $(N_p)_4$ and the two $C_{20}N_4$ planes is a direct measure of the "doming", the saucerlike deformation of the macrocycle that is necessary to improve the overlap of the donor pairs of the eight N_p atoms with the acceptor sites of the large

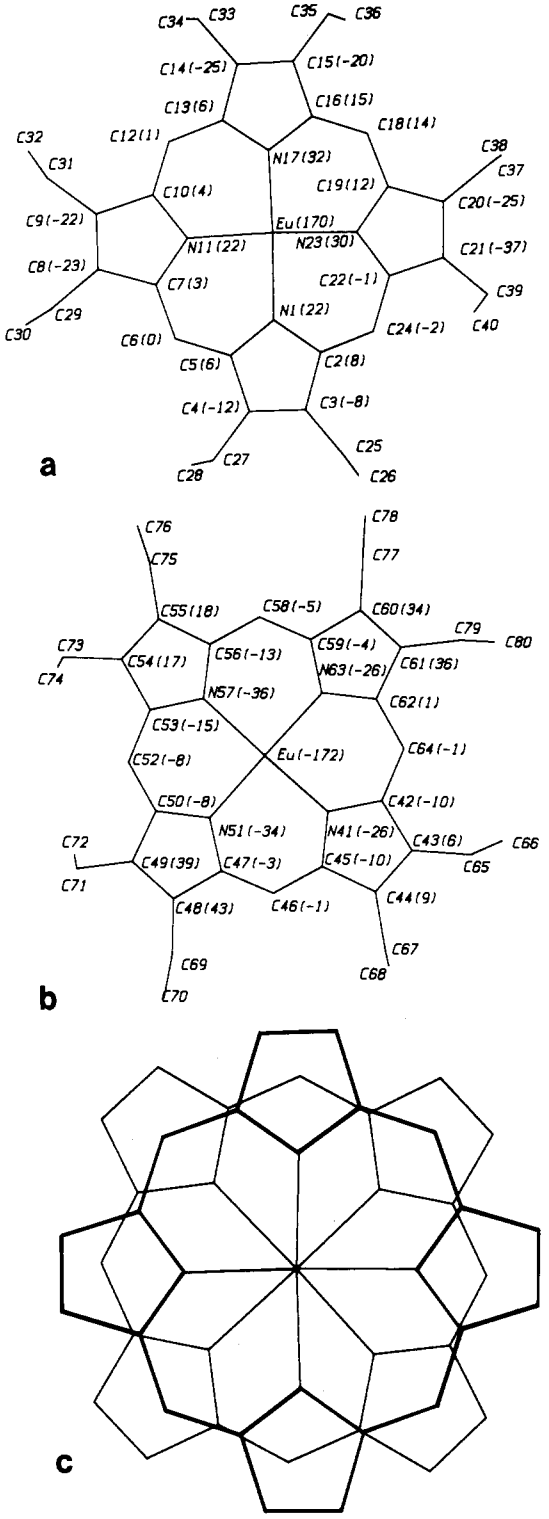

Figure 5. Stick bond model projections of parts of the $Eu(OEP)_2$ molecule in **2**: (a, b) projections along the Ct1–Eu and Eu–Ct2 axes (Ct1 and Ct2 are the centroids of the $(N_p)_4$ atoms; the labeling scheme of the crystallographically independent porphyrin atoms is given; also shown are the deviations of the porphyrin core atoms (in 0.01 Å units) from their respective mean planes); (c) projection along the Ct1–Ct2 axis showing the respective rotations of the two superimposed macrocycles omitting the ethyl groups.

central metal ions which cannot sit in the center of a single porphyrinate ligand. This leads to the conclusion that the doming decreases as the ionic radius of the Ln ion increases, reflecting a decrease in covalent bonding. In detail, the extent of doming can be taken from the inclinations of the pyrrole rings, which are expressed by the dihedral angles subtended between the mean plane of a specific pyrrole ring and the $(N_p)_4$ plane to which it belongs. The average inclinations show the same tendency as the D_5 values in Table III.

Table V. Molar Magnetic Susceptibilities (χ_{met}) of the Metal Ion in **2** (emu/mol) as a Function of Temperature and Other Data (emu) of the Magnetic Measurements[a]

T, K	$10^6\chi_g$	$10^3\chi_{mol}$	$10^3\chi_{met}$	μ_{eff}, μ_B
2.6	64.21	78.20	79.10	1.28
4.0	50.42	61.40	62.30	1.41
8.0	25.49	31.00	32.00	1.43
14.8	18.24	22.20	23.20	1.66
18.0	13.96	17.00	18.00	1.61
27.7	10.42	12.70	13.60	1.74
37.0	8.832	10.80	11.70	1.86
45.3	7.976	9.71	10.70	1.97
54.0	7.358	8.95	9.92	2.07
68.0	6.62	8.06	9.02	2.22
79.0	6.243	7.60	8.56	2.33
90.6	5.946	7.24	8.20	2.44
112.8	5.540	6.75	7.70	2.64
123.0	5.376	6.54	7.51	2.72
139.8	5.109	6.22	7.18	2.84
161.8	4.863	5.92	6.88	2.99
179.6	4.689	5.71	6.67	3.10
201.5	4.388	5.34	6.30	3.19
231.1	4.166	5.07	6.03	3.34
268.3	3.766	4.59	5.55	3.45
301.9	3.481	4.24	5.20	3.55

[a] Mol wt 1217.52; χ_{mol} for the diamagnetic correction is 0.96×10^{-3} emu/mol.

Conclusion. As to the serious problem of understanding the electron distribution in $Eu(OEP)_2$ (**2**), neither the spectroscopic nor the structural evidence at −100 °C allows a distinction of the two porphyrin ligands. The presence of two porphyrin ligands with the distinct negative charges −1 and −2 should cause different Eu–N bond lengths in the two porphyrin systems, a situation that is reminiscent of the situation in the triple-deckers.[18] However, the small differences quoted in Table II are not significant. Therefore, at −100 °C, there is either statistical disorder of two porphyrin ligands in different oxidation states or complete delocalization of the hole between the two cofacial π-electron systems of the porphyrin ligands. We are hoping to shed more light on the electron distribution by ESR investigations of $Y(OEP)_2$[35] and $Lu(OEP)_2$.[37]

Acknowledgment. This work was supported by the Deutsche Forschungsgemeinschaft (Bonn, FRG), the Centre National de la Recherche Scientifique (Paris, France), the Fonds der Chemischen Industrie (Frankfurt, FRG), and the Vereinigung von Freunden der Technischen Hochschule Darmstadt. J.W.B. is grateful for having been Professor Associé at the Université Louis Pasteur, Strasbourg, France, in 1984. We thank Professor Dr. B. Elschner and D. Flasche and N. Preusse for magnetic and ESR measurements, Priv.-Doz. Dr. M. Veith and M. Fischer for the mass spectrum, and Dr. S. Braun for advice on the measurement of the NMR spectra.

Registry No. **2**, 96383-14-1; **4**, 96383-18-5; $Na[Eu(OEP)_2]$, 111525-85-0; $Eu(acac)_3$, 14284-86-7.

Supplementary Material Available: Tables of isotropic thermal parameters, hydrogen atom parameters, complete bond distances, and complete bond angles for **2** (12 pages); a table of observed and calculated structure factor amplitudes for **2** (34 pages). Ordering information is given on any current masthead page.

(37) Petit, P.; Turek, P.; Andrē, J. J.; Buchler, J. W.; Kihn-Botulinski, M.; De Cian, A.; Simon, J., manuscript in preparation.